Protective Effect of Dexpanthenol on Ischemia-Reperfusion-Induced Liver Injury

M. Ucar[a], M.S. Aydogan[a,*], N. Vardı[b], and H. Parlakpınar[c]

[a]Department of Anesthesiology, Faculty of Medicine, Inonu University, Turkey; [b]Department of Histology-Embryology Faculty of Medicine, Inonu University, Turkey; and [c]Department of Pharmacology, Faculty of Medicine, Inonu University, Turkey

ABSTRACT

Objective. We aimed to investigate the protective and therapeutic effects of dexpanthenol (DXP) on liver injuries induced by ischemia-reperfusion (IR) in an in vivo rat model.

Methods. Thirty-two rats were randomly divided into 4 experimental groups (n = 8 in each group: Sham, IR, DXP, and DXP+IR. DXP (500 mg/kg) was intraperitoneally administered for 30 min before 60 min of ischemia, followed by 60 min of reperfusion to rats in the DXP and DXP+IR groups. All rats were euthanized on day 10 to evaluate immunohistopathological changes as well as tissue levels of oxidants and antioxidants.

Results. IR decreased total glutathione (tGSH) levels in IR group when compared to the Sham group. DXP supplementation to IR group significantly ameliorated tGSH levels ($P < .05$). IR also elevated myeloperoxidase production compared to the Sham group, whereas DXP treatment prevented these hazardous effects. However, plasma superoxidedismutase, catalase, and malondialdehyde levels did not differ between the DXP+IR than the IR rats. Histologic tissue damage was reduced in the DXP and DXP+IR group.

Conclusion. Liver IR is an inevitable problem during liver surgery. Our results suggested that DXP pretreatment suppressed oxidative stress and increased antioxidant levels in a rat model of liver IR.

ISCHEMIA-REPERFUSION (IR) injury (IRI) is associated with various clinical conditions, such as myocardial and brain infarction, major trauma, shock, and surgery under vascular occlusion [1]. Liver ischemia-reperfusion (IR) injury is one of the main causes of hepatic failure. Temporary clamping of the portal triad, a common strategy to minimize bleeding during liver surgery, produces hepatic IRI that may result in postoperative liver dysfunction with adverse effects on graft liver transplant function [2,3].

Liver IRI is associated with a number of processes, such as activation of Kupffer cells, production of reactive oxygen species (ROS), neutrophil infiltration, and an increase in the levels of adhesion molecules, release of cytokines, hepatocyte injury, and separation of sinusoidal endothelial cells. It has been reported in literature that pharmacologic agents such as antioxidants, anti-inflammatory agents, and vasodilators together with ischemic preconditioning have been used to treat IRI [4].

Dexpanthenol (D-panthenol;(+)-2,4-dihydroxy-N-(3-hydroxypropyl)-3,3 dimethylbutyramide) (DXP), an alcoholic analogue of pantothenic acid (PA), also known as provitamin B5, is oxidized to PA inside the tissues [5]. It is well established that PA and its derivatives increase the level of reduced glutathione (GSH), Coenzyme A (Co A) (especially mitochondrial Co A) and adenosine-5'-triphosphate (ATP) synthesis within the cell [6]. In this way, it supports epithelization, anti-inflammatory, and antioxidant activities, all of which play a major role in cellular defense and in the repair systems against oxidative stress and the inflammatory response [7].

This experimental study was designed to investigate the protective and therapeutic effects of DXP on liver injury induced by IR in an in vivo rat model. Immunohistopathological findings, including apoptotic changes, were evaluated along with biochemical analyses carried out

*Address correspondence to Mustafa Said Aydogan, MD, Department of Anesthesiology and Reanimation, Inonu University School of Medicine, Malatya, Turkey. Tel: +904223410660-3160; Fax: +904223410728. E-mail: dr_mustafasaid@hotmail.com

230 Park Avenue, New York, NY 10169

0041-1345/18
https://doi.org/10.1016/j.transproceed.2018.07.012

Table 1. The Biochemical Results

Group	Sham	DXP	IR	DXP+IR
tGSH	16.70 ± 8.30	14.26 ± 5.64	7.63 ± 2.72*	18.53 ± 4.27†
MPO	32.95 ± 9.46	29.04 ± 6.85	57.20 ± 17.75‡	43.81 ± 4.53
MDA	30.42 ± 4.71	30.64 ± 5.60	34.95 ± 3.43	32.44 ± 3.57
SOD	44.26 ± 2.52	45.63 ± 2.49	41.41 ± 1.94	43.53 ± 1.74
CAT	180.0 (154.2–187.9)	298.9 (260.7–315.6)	183.6 (168.1–204.1)	191.5 (177.1–315.5)

Abbreviations: CAT, catalase; DXP, dexpanthenol; IR, ischemia-reperfusion; MDA, malondialdehyde; MPO, myeloperoxidase; SOD, superoxidedismutase; tGSH, total glutathione.
*Significant decrease ($P < .05$) vs sham group.
†Significant increase ($P < .05$), vs IR group.
‡Significant increase ($P < .05$), vs sham group.

for the determination of tissue malondialdehyde (MDA), superoxidedismutase (SOD), myeloperoxidase (MPO), catalase (CAT), and total glutathione (tGSH) levels in order to examine these effects.

MATERIALS AND METHODS

Animals

A total of 32 Sprague-Dawley female rats (10–12 weeks old) weighing between 250–300 g were obtained from our Laboratory Animal Research Center. The rats were maintained at 21 ± 2°C with a relative humidity of 60 ± 5% under 12-hour light/dark cycles. They were housed in plastic cages (50 × 35 × 20 cm; 8 animals per cage). The experiments were performed according to the standards of animal research of the National Health Research Institute and with the approval of our University Ethical Committee.

Experimental Design

The rats were randomly divided into 4 groups, each consisting of 8 animals. Group 1, the Sham group, underwent exposure of the hepatic artery, portal vein, and bile duct region but no IR. Group 2, the IR group, underwent 60 min of ischemia followed by 60 min of reperfusion. Group 3, the DXP group, underwent 500 mg/kg DXP (500 mg Bepanthene ampul, Bayer Corp., Leverkusen, Germany) given intraperitoneally. Group 4, the DXP+IR group, underwent 500 mg/kg DXP given intraperitoneally 30 min before 60 min of ischemia, followed by 60 min of reperfusion. The dosages of DXP were chosen according to previous dose-response studies [8,9].

Surgical Procedure

Following a 12-hour fast, the rats were anesthetized with intraperitoneally administered ketamine (40 mg/kg) and xylazine (10 mg/kg). The abdominal region was sterilized with povidine-iodine solution and explored through a midline laparotomy using minimal dissection. Only midline laparotomy was performed for the Sham group; the abdomen was closed without any further procedure. In the IR and DXP+IR groups, total hepatic ischemia was induced for 60 min by occluding the hepatic artery, portal vein, and bile duct using a non-traumatic vascular clamp. The liver was reperfused for 60 min after removing the clamp. After declamping, we confirmed restored hepatic blood flow before closure of the incision. During the surgery, body temperature was maintained at approximately 37.5°C with a heating lamp. Fluid loss was replaced by intraperitoneal injection of 3 ml warm (37°C) saline before abdominal closure. After 60 min of reperfusion, the abdomen was reopened, and 3 ml blood was drawn from the heart into heparinized microcentrifuge tubes. Subsequently, the animals were euthanized to perform a hepatectomy. The plasma and liver tissues were stored at −80°C for biochemical analyses. At the same time, hepatic tissue was stored in 10% formalin for histologic examination. All coded specimens were evaluated by individuals blinded to the group assignments.

Homogenization

Tissues were homogenized using an in ice-cold phosphate buffered saline (PCV Kinematica Status Homogenizator, pH 7.4). The homogenate was sonified with an ultrasonifier in 3 cycles (20-s sonications with a 40 s pause on ice). The homogenate was centrifuged (15,000 *g*, 10 min, 4°C) and a cell-free supernatant was immediately subjected to an enzyme assay. For lipid peroxidation analysis, the tissue was washed 3 times with ice-cold 0.9% NaCl solution and homogenized in 1.15 KCl. The homogenates were immediately subjected to a lipid peroxidation assay.

Determination of Enzyme Activities

The enzymes catalase (CAT), superoxide dismutase (SOD), and myeloperoxidase (MPO) activity were determined spectrophotometrically. CAT activity was measured at 37°C by following the rate of disappearance of H_2O_2 at 240 nm ($\varepsilon_{240} = 40 = 40\ M^{-1}\ cm^{-1}$) [10]. One unit of catalase activity was defined as the amount of enzyme catalyzing the degradation of 1 μmol of H_2O_2/min at 37°C. CAT activity was expressed as U/mg protein in the tissue.

SOD (Cu, Zn-SOD) activity in the supernatant fraction was measured using the xanthine oxidase/cytochrome c method [11], where 1 unit (U) of activity was the amount of enzyme needed to cause half-maximal inhibition of cytochrome c reduction. The amount of SOD in the extract was determined as U of enzyme mg-1 protein, using a commercial SOD as the standard.

For MPO activity, samples were weighed at 0.1 g and put into 1 mL of phosphate buffer (50 mM, pH 6) and all tissues were homogenized under ice with an IKA-Werke T25 homogenizer. The homogenates were then centrifuged with Hettich Universal 320 microcentrifuge at 15,000 *g* for 15 min at 40°C (Hettich Universal 320). The pellets were separated from the supernatant and added to 500 μL of HETAB solution (0.5% w/w in 50 mM, pH 6 phosphate buffer). The solutions were allowed to freeze-thaw twice and subjected to sonication for a period of 15 seconds in a VCX 130 (Sonics & Materials, Newtown,

Table 2. The Biochemical Results

Groups	tGSH	MPO	MDA	CAT	SOD
Sham-IR	0.043	0.033	0.170	0.290	0.088
IR-DXP+IR	0.000	0.363	0.686	0.649	0.143

Abbreviations: CAT, catalase; DXP, dexpanthenol; IR, ischemia-reperfusion; MDA, malondialdehyde; MPO, myeloperoxidase; SOD, superoxidedismutase; tGSH, total glutathione.

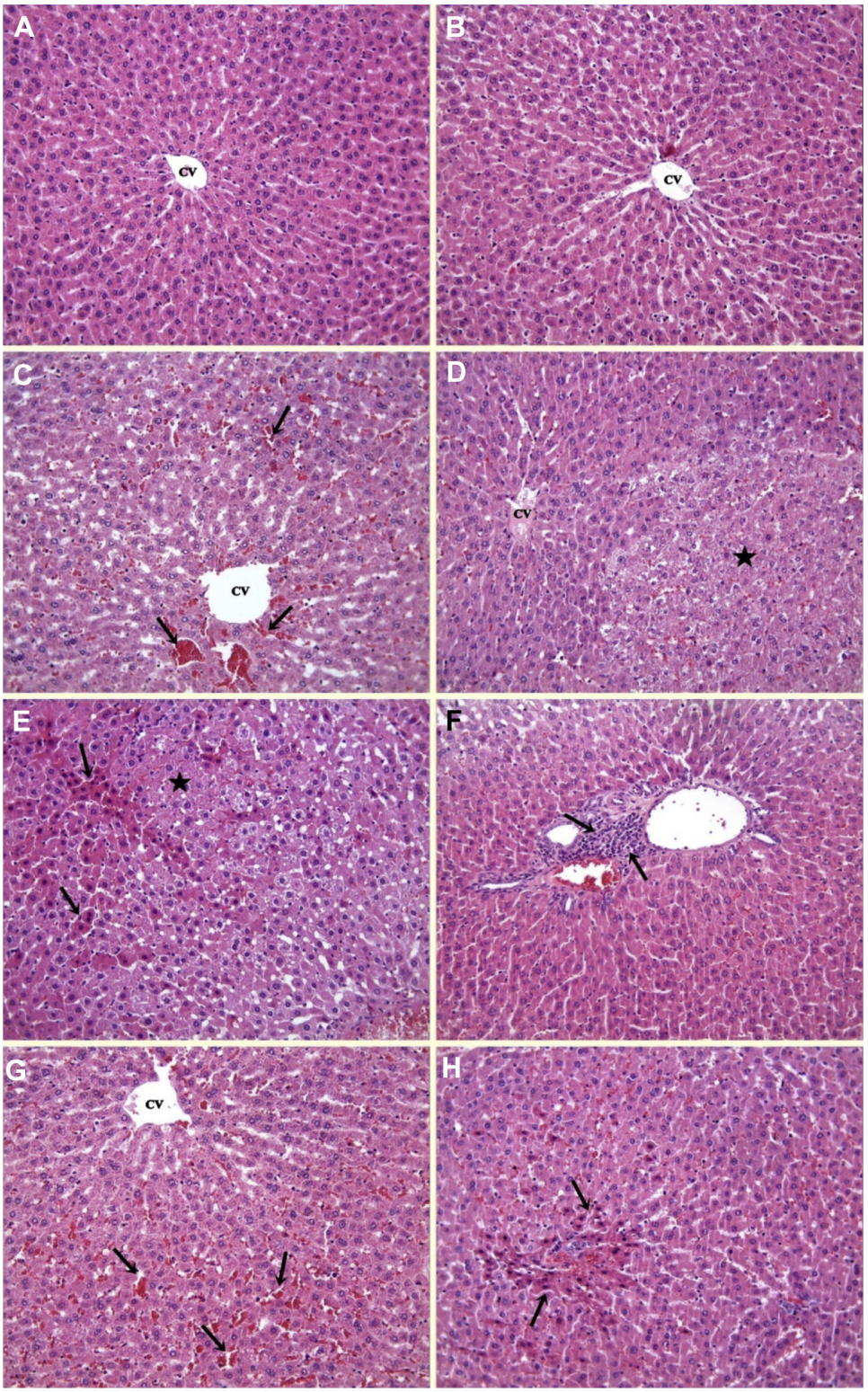

Fig 1. **(A)** (Sham) and **(B)** (DXP) groups: The normal histological appearance of the liver. Hepatocytes cordons radially localize around central vein (CV). **(C)** (IR group): Congestion is evident (arrows). **(D)** (IR group): appearance of necrotic areas (star). **(E)** (IR group): Hepatocytes with dense eosinophilic cytoplasm and pyknotic nucleus (arrows) and necrotic area (star). **(F)** (IR group): Infiltration is seen in the portal area (arrows). **(G)** (DXP+IR group): Congestion (arrows) is still present. **(H)** (DXP+IR group): Decreased density of hepatocytes with eosinophilic cytoplasm (arrows) according to the IR group (H&E × 20).

Conn, United States). The samples were then centrifuged at 15,000 *g* for 15 min. Twenty-five µL of supernatant and 200 µL of reaction mixture (0.167 mg/ml o-Dianisidine and 0.0005% v/v hydrogen peroxide in 50 mM phosphate buffer, pH: 6) were added into 96 well plates, and the measurement was performed at a wavelength of 460 nm with a BioTek Eon Eliza microplate reader (BioTek, Loughborough, UK). MPO activity results were given in unit per gram of wet tissue [12].

Total Glutathione (tGSH) Assay

The formation of 5-thio-2-nitrobenzoate (TNB) was followed spectrophotometrically at 412 nm [13]. The amount of tGSH in the extract was determined as nmol/mg protein by using a commercial GSH as the standard.

MDA Assay

As a marker of lipid peroxidation production, the MDA concentration was measured as described by Buege and Aust [14] with a minor modification. The reaction mixture was prepared by adding 250 µL of homogenate to 2 mL of reaction solution (15% trichloroacetic acid: 0.375% thiobarbituric acid: 0.25 N HCl, 1:1:1, w/v) and heated at 100°C for 30 min. The mixture was cooled to room temperature, centrifuged at 10,000 *g* for 10 min, and the absorbance of the supernatant was recorded at 532 nm. MDA results were expressed as nmol/mg protein in the homogenate.

Determination of Protein

Protein levels in the tissue samples were measured using the Bradford method [15]. The absorbance measurement was taken at 595 nm using a UV-VIS spectrophotometer. Bovine serum albumin (BSA) was used as the protein standard.

HISTOPATHOLOGICAL ANALYSIS

Liver tissue was fixed in 10% formalin and embedded in paraffin. Tissue sections were cut at 4 µm, mounted on slides, stained with hematoxylin and eosin (H&E) for general liver structure, and subjected to periodic acid schiff (PAS) to demonstrate the glycogen deposition in hepatocytes and Kupffer cells. The liver damage was semi-quantitatively assessed as follows: hepatocytes with eosinophilic cytoplasms and pyknotic nuclei, necrosis, inflammatory cell infiltration, sinusoidal congestion, and loss of the glycogen deposition in hepatocytes.

Ten fields were examined in X20 objective magnification for each criterion. Accordingly, the extent of liver damage was scored between 0–3; 0 was defined as a normal liver, 1 was defined as liver damage involving $\leq 25\%$ of the liver, 2 was defined as liver damage involving 25–50% of the liver, and 3 was defined as liver damage involving $\geq 50\%$ of the liver.

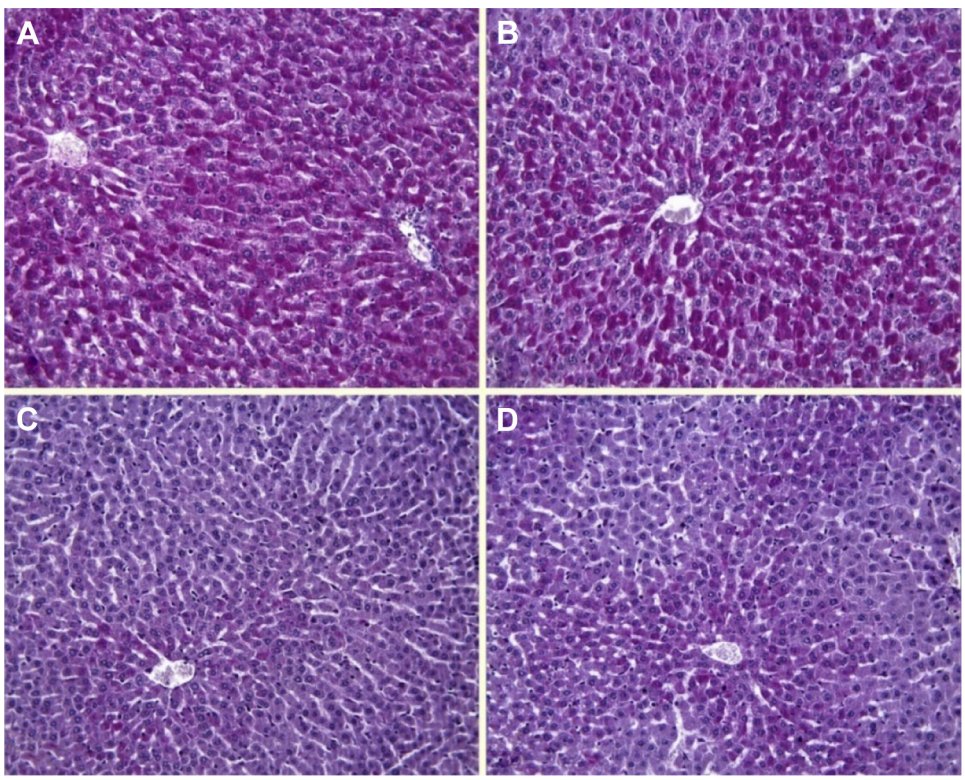

Fig 2. **(A)** (Sham) and **(B)** (DXP) groups: The hepatocyte cytoplasms containing glycogen are stained magenta in sections. **(C)** (IR group): Marked decreasing glycogen storage in hepatocytes. **(D)** (DXP+IR group): The view of glycogen content in hepatocytes cytoplasm (PAS × 20).

In addition, Kupffer cells were counted manually on digital images Leica Q Win analysis system using point counting. Three sections were used for each animal. Ten fields were randomly chosen at × 40 magnification for each section, reaching a total of 30 fields per animal.

IMMUNOHISTOLOGICAL ANALYSIS

Tissue sections 4 μm thick were deparaffinized, rehydrated, placed in an antigen retrieval solution (citrate buffer, pH 6.0), boiled in a pressure cooker for 20 minutes, and cooled to room temperature for 20 min. The sections were then washed with phosphate-buffered saline (PBS, pH 7.4). To block endogenous peroxidase activity, the slides incubated in 0.3% hydrogen peroxide solution for 15 min at room temperature and washed in PBS. After the blocking of non-specific antigen-binding sites with a protein block, primer antibodies caspase-3 and Ki-67 (Thermo Fisher Scientific, Loughborough, UK) were applied for 60 minutes at room temperature. After being rinsed with PBS, sections were incubated with biotinylated secondary antibody and streptavidin peroxidase for 10 minutes at room temperature. Samples were visualized with the chromogenic substrates AEC, counterstained with hematoxylin, and mounted in glass slide. The caspase-3 and Ki-67 kit was used according to the manufacturer's instructions.

Nuclei of Ki-67 positive cells were stained brown. Stained hepatocyte nuclei with Ki-67 were counted manually on digital images using the Leica Q Win analysis system (Leica Micros Imaging Solutions, Cambridge, UK) and point counting. Three sections were used for each animal. Ten fields were randomly chosen at x40 magnification for each section, reaching a total of 30 fields per animal.

STATISTICAL ANALYSIS

Data were analyzed using the SPSS software program for Windows ver. 17.0 (IBM, Armonk, NY). The data were expressed as either median (min-max) values or mean ± standard deviation (SD) depending on the overall variable distribution. The normality of the distribution was confirmed using the Shapiro-Wilk test. The normally distributed data were analyzed using a one-way ANOVA followed by the Tamhane T2 test. The non-normally distributed data were compared using the Kruskal-Wallis H test on the different groups. When significant differences were determined, multiple comparisons were carried out using the Mann-Whitney U test with the Bonferroni

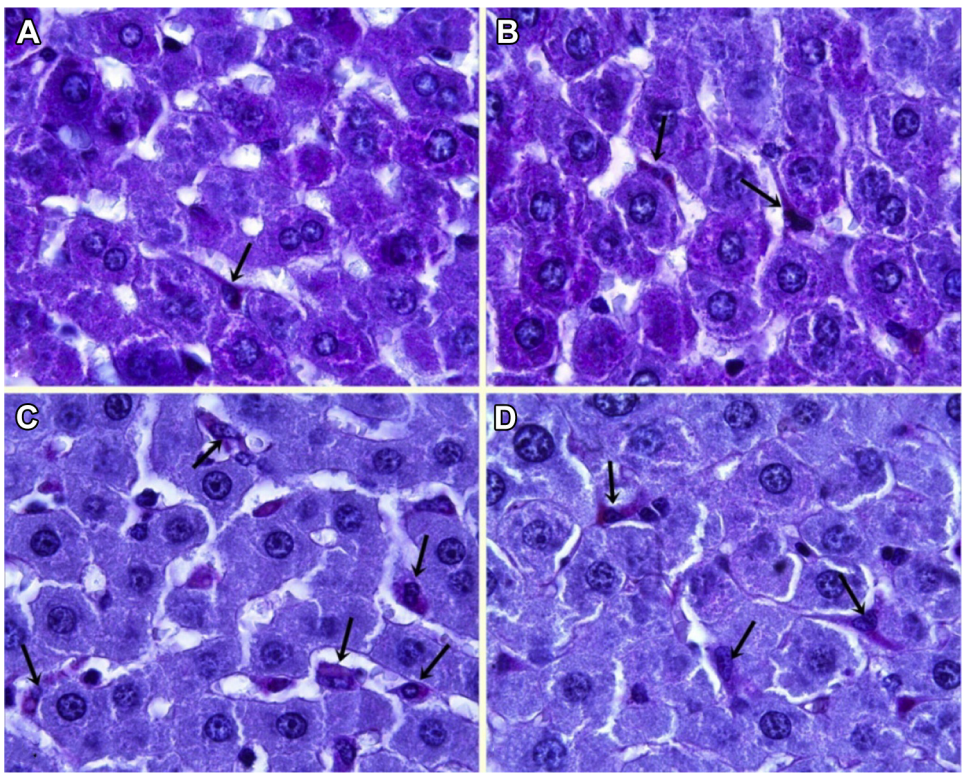

Fig 3. **(A)** (Sham) and **(B)** (DXP) groups: PAS positive reaction show a magenta staining in which Kupffer cells is present in the lumen or near the wall of sinusoid (arrows). **(C)** (IR group): Note to increasing the number of Kupffer cells (arrows). **(D)** (DXP+IR group): Decreased number of Kupffer cells (arrows) according to IR group (PAS × 100).

correction. The results were expressed as the med (min-max). P values $< .05$ were considered significant.

RESULTS

Biochemical

The biochemical results are presented in Tables 1 and 2. In brief, IR decreased tGSH levels in the IR group compared to the Sham group. DXP supplementation to IR group significantly ameliorated t GSH levels ($P < .05$). IR also elevated MPO production compared to the Sham group, whereas DXP treatment prevented these hazardous effects. However, plasma SOD, CAT, and MDA levels did not differ between the DXP+IR compared to the IR rats.

Histopathological

The sections stained with H&E drawn from the sham and DXP groups showed a normal appearance of the liver histology except minimal changes (Figs 1A, 1B). The appearance of the sinusoids among the hepatocyte cordons was normal. On the other hand, in the IR group, most prominent change was sinusoidal congestion (Fig 1C). Limited necrotic areas were observed in some lobules (Fig 1D). Another finding was the hepatocytes with eosinophilic cytoplasms and pyknotic nuclei (Fig 1E). The focus of infiltration in the portal area was also detected in this group (Fig 1F). Although the score of histologic damage was observed as attenuated in the DXP+IR group, some degenerative changes were still present, such as congestion and infiltration (Fig 1G). However, the density of the hepatocytes with eosinophilic cytoplasms and pyknotic nuclei decreased significantly in the DXP+IR group compared to the IR group (Fig 1H) ($P < .05$). There was no necrosis in this group.

The sections stained with PAS staining method, the hepatocyte cytoplasms containing glycogen, and the Kupffer cells were dyed magenta in the Sham and DXP groups (Figs 2A, 2B). The Kupffer cells were observed in the lumen or near the wall of sinusoid (Figs 3A, 3B). The glycogen storage in hepatocytes was detected as decreased in the IR group compared to controls (Fig 2C) ($P < .05$). The increase in the number of Kupffer cells were found to be statistically significant in the IR group compared to that of the sham group (Fig 3C) ($P < .05$). On the other hand, DXP treatment significantly reduced the loss of glycogen in the hepatocytes (Fig 2D) ($P < .05$). Furthermore, the number of Kupffer cells was determined to have decreased in the DXP+IR group compared to IR group (Fig 3D) ($P < .05$).

Immunohistological

In the Ki-67 immunostain, the number of positive hepatocytes decreased at a statistically significant level in the IR and DXP+IR groups (Figs 4C, 4D) compared to the Sham and DXP groups (Figs 4A, 4B) ($P < .05$). On the other hand, the DXP+IR group was statistically similar to the IR

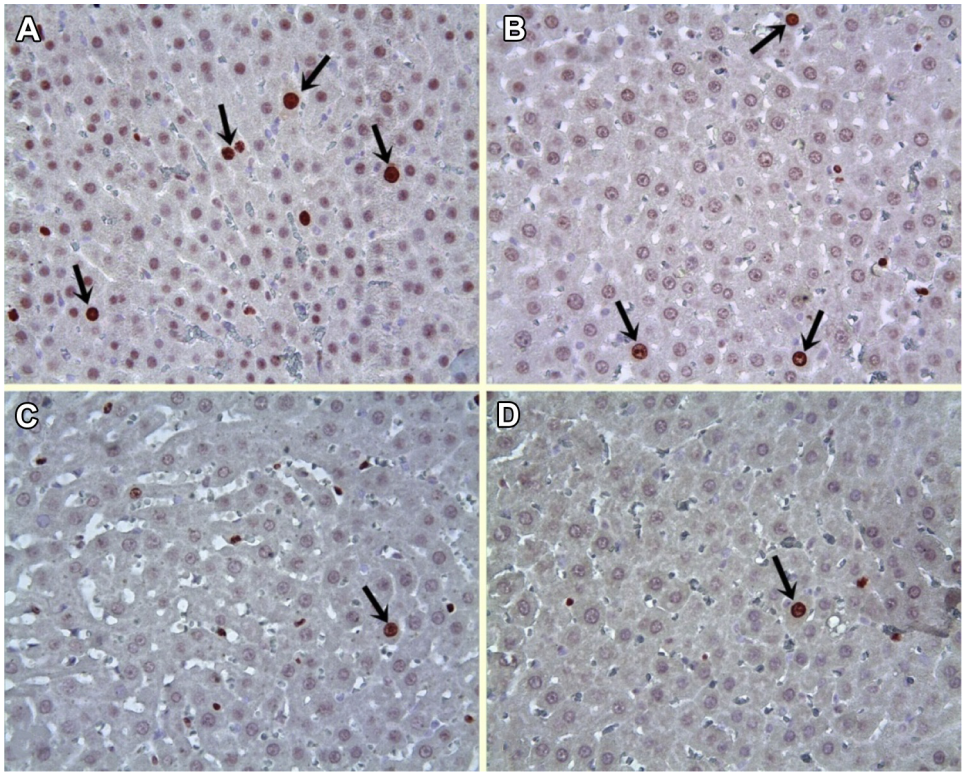

Fig 4. Arrows show the number of Ki-67 positive hepatocytes. **(A)** Sham group; **(B)** DXP group; **(C)** IR group; **(D)** DXP+IR group (x 40).

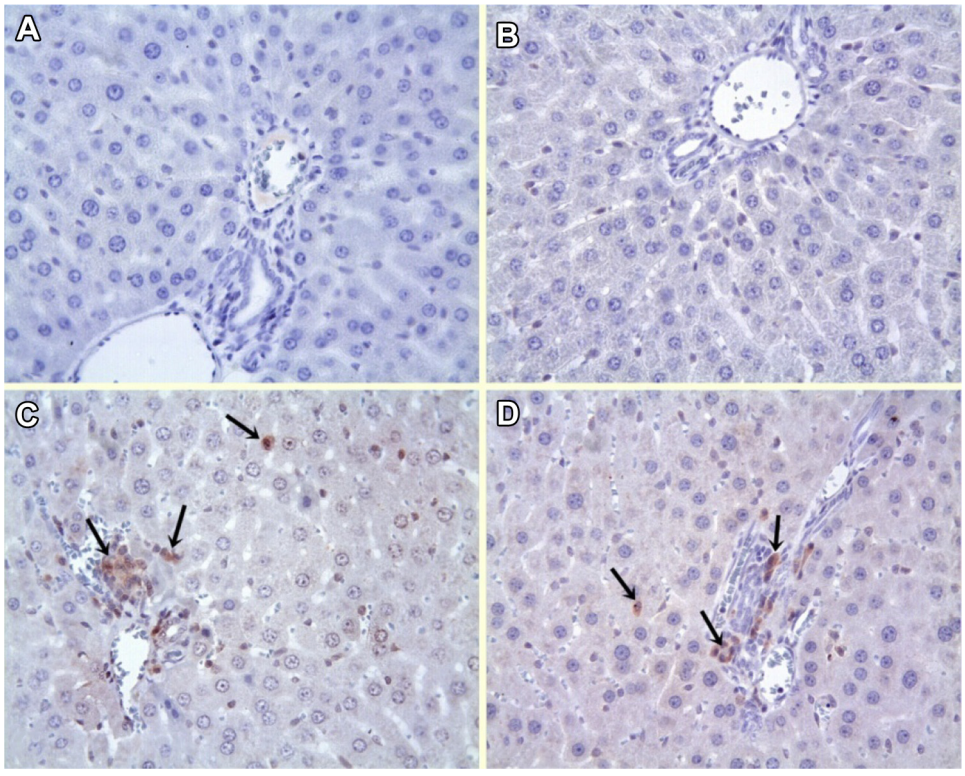

Fig 5. **(A)** (Sham) and **(B)** (DXP) groups; caspase-3 positive cells are not observed. **(C)** IR and **(D)** (DXP+IR) groups: caspase-3 positive cells (arrows) are seen only at portal areas and on the wall of the sinusoid. Notice hepatocytes are not stained with caspase-3 in any groups (caspase-3 × 40).

group in terms of the number of Ki-67 positive cells ($P > .05$). In the sections stained with caspase-3, there were no caspase-3 positive hepatocytes in any of the groups. However, caspase-3 positive cells were observed at portal areas and on the wall of the sinusoid in the IR and DXP+IR groups (Fig 5). The results of histopathological score and number of Kupffer and Ki-67 positive cells in all groups are presented in Table 3.

DISCUSSION

The main finding of the present study was that DXP may protect against liver IRI. In this study, we found that IR caused an increase in the MDA level and a decrease in the SOD and tGSH activities in liver tissue. However, the administration of DXP to the IR group reduced the MDA level while increasing SOD and tGSH activity. The structural changes in the liver due to IR were reversed via DXP. These findings indicated that 500 mg/kg dose of DXP protected against IR-induced damage in IR rat models.

Liver IR is inevitable during liver surgery, including transplantation and tumor resection [16]. The extent of IR-associated liver injury is a major factor directly affecting graft survival and function. Both cold and warm ischemia occurs during transplantation; we used warm ischemia in our surgical protocol. Evidence shows that ROS play a key

Table 3. The Results of Histopathological Score and Number of Kupffer and Ki-67 Positive Cells in All Groups

Group	Sham	DXP	IR	DXP+IR
Congestion	0.0 (0.0–2.0)	0.0 (0.0–2.0)	2.0 (0.0–3.0)*	2.0 (0.0–3.0)
Infiltration	0.0 (0.0–2.0)	0.0 (0.0–1.0)	1.0 (0.0–2.0)*	0.5 (0.0–2.0)
Hypereosinophilic hepatocyte	0.0 (0.0–1.0)	0.0 (0.0–1.0)	0.0 (0.0–2.0)*	0.0 (0.0–2.0)†
Necrosis	0.0 (0.0–0.0)	0.0 (0.0–0.0)	0.0 (0.0–3.0)*	0.0 (0.0–0.0)†
Glycogen loss	0.0 (0.0–1.0)	0.0 (0.0–2.0)	3.0 (1.0–3.0)*	2.0 (0.0–3.0)†
Kupffer cells	2.0 (2.0–10.0)	5.0 (2.0–15.0)	14.0 (4.0–32.0)*	9.0 (2.0–25.0)†
Ki-67 positive hepatocyte	1.0 (0.0–5.0)	1.0 (0.0–4.0)	0.0 (0.0–4.0)‡	0.0 (0.0–4.0)‡

Abbreviations: DXP, dexpanthenol; IR, ischemia-reperfusion.
*Significant increase ($P < .05$) vs sham group.
†Significant decrease ($P < .05$) vs DXP + IR group.
‡Significant increase ($P < .05$) vs sham group.

role in liver IR injury [17]. One class of molecules that is affected negatively by the ROS associate with IR injury includes lipids. ROS causes lipid peroxidation, which eventually leads to membrane injury, alterations in ion permeability and enzyme activity, and ultimately cell death. Simultaneously, the inflammatory process begins, significantly increasing the severity of injury.

Lipid peroxidation is the process of cell damage, and cell death is a common consequence of this process. The end product of lipid peroxidation is MDA, which acts as an indicator of oxidative damage. Because of the cross-link formation and interaction with membrane lipids, MDA leads to severe damage [18]. In many studies, DXP was reported to prevent cell damage produced by lipid peroxidation, irrespective of the source of oxidative stress [19–22]. Consistent with the literature, after administration of DXP, MDA levels are reduced following acetaminophen toxicity and cardiovascular and renal damage [23–25]. It was observed in the present study that MDA levels increased after IRI; however, they were similar to control values after DPX treatment. The findings indicating that the MDA level increased in the IR group and decreased in the DPX group are consistent with those of our study.

SOD and GPx have been widely studied among endogenous antioxidants. SOD catalyzes the dysmutation of superoxide anion to hydrogen peroxide and oxygen, but hydrogen peroxide still produces liver oxidative injury. GPx further catalyzes the transformation of hydrogen peroxide to form water [26]. In many reports, however, SOD activity was not affected, suggesting that this enzyme is a less sensitive predictor of oxidative stress [27,28]. DPX and its derivatives play a part in the disposal of ROS by increasing GPX; they also repair cell membranes and tissue injuries by increasing CoA and ATP synthesis, which produce phospholipids and cholesterol in the cell [26]. We observed that DPX pretreatment did not increase SOD and GPx activities in the IR-DPX group, which may be due to DPX indirectly reducing oxidative damage. However, further investigations are needed to understand the liver mechanism(s).

The histologic investigation suggested that IR caused severe pathological alterations in the liver, including edema, sinusoidal congestion, eosinophilic cytoplasms, and pyknotic nuclei. In addition, glycogen storage in hepatocytes was detected as decreased in the IR group, and the number of Kupffer cells was found to have increased to a statistically significant level. DXP treatment reduced the density of the hepatocytes with eosinophilic cytoplasms, pyknotic nuclei loss, and glycogen in the hepatocytes. In addition, the number of Kupffer cells was found to have decreased in this group. On the other hand, DXP treatment group was statistically similar to the IR group in terms of Ki-67 count and caspase-3-positive cells.

According to our findings, which paralleled the histopathological and immunohistological evidence, administration of DXP abolished certain I/R injury effects, such as the decreased level of GPX or the increased levels of MDA.

CONCLUSION

There were some limitations of the study. The first limitation was that the sample size was small. Secondly, DXP-dose-related or longer time-dependent responses to IR injury were not evaluated. However, DXP-attenuated IR injury was established even if it was an incomplete protection.

The beneficial effects of DXP on liver IR injury were evaluated for the first time in this study. DXP administered at a dose of 500 mg/kg given intraperitoneally during the ischemic period ameliorated the liver damage that occurred after IR injury. The beneficial changes in biochemical parameters, including antioxidant status, were also associated with parallel changes in both histopathological and immunohistological appearance of the tissue.

It is well established that DXP exerts very powerful free radical scavenger and antioxidant effects during in vivo and in vitro studies. In the current study, it is possible to say that, according to our biochemical and histopathological results, DXP has beneficial effects on IR injuries at the tissue level because of its antioxidant, anti-inflammatory, and ROS scavenger properties.

REFERENCES

[1] Abu-Amara M, Yang SY, Tapuria N, Fuller B, Davidson B, Seifalian A. Liver ischemia/reperfusion injury: processes in inflammatory networks—a review. Liver Transpl 2010;16:1016–32.

[2] Aydogan MS, Yucel A, Erdogan MA, Polat A, Cetin A, Ucar M, et al. Effects of oral β-glucan on liver ischemia/reperfusion injury in rats. Transplant Proc 2013;45:487–91.

[3] Tüfek A, Tokgöz O, Aliosmanoglu I, Alabalik U, Evliyaoglu O, Çiftçi T, et al. The protective effects of dexmedetomidine on the liver and remote organs against hepatic ischemia reperfusion injury in rats. Int J Surg 2013;11:96–100.

[4] Ermis H, Parlakpinar H, Gulbas G, Vardi N, Polat A, Cetin A, et al. Protective effect of dexpanthenol on bleomycin-induced pulmonary fibrosis in rats. Naunyn Schmiedebergs Arch Pharmacol 2013;386:1103–10.

[5] Ceylan H, Yapici S, Tutar E, Ceylan NO, Tarakçıoğlu M, Demiryurek AT. Protective effects of dexpanthenol and y-27632 on stricture formation in a rat model of caustic esophageal injury. J Surg Res 2011;171:517–23.

[6] Cagin YF, Atayan Y, Sahin N, Parlakpinar H, Polat A, Vardi N, et al. Beneficial effects of dexpanthenol on mesenteric ischemia and reperfusion injury in experimental rat model. Free Radic Res 2016;50:354–65.

[7] Turgut O, Ay AA, Turgut H, Ay A, Kafkas S, Dost T. Effects of melatonin and dexpanthenol on antioxidant parameters when combined with estrogen treatment in ovariectomized rats. Age (Dordr) 2013;35:2229–35.

[8] Etensel B, Ozkisacik S, Ozkara E, Karul A, Oztan O, Yazici M, et al. Dexpanthenol attenuates lipid peroxidation and testicular damage at experimental ischemia and reperfusion injury. Pediatr Surg Int 2007;23:177–81.

[9] Li-Mei W, Jie T, Shan-He W, Dong-Mei M, Peng-Jiu Y. Anti-inflammatory and anti-oxidative effects of dexpanthenol on lipopolysaccharide induced acute lung injury in mice. Inflammation 2016;39:1757–63.

[10] Luck H. Methods of enzymatic analysis. Weinheim/Bergstr., Germany: Verlag Chemie Academic Press; 1963.

[11] McCord JM, Fridovich I. Superoxide dismutase: an enzymatic function for erythrocuprein (hemocuprein). J Biol Chem 1969;44:6049–55.

[12] Hillegas LM, Griswold DE, Brickson B, Albrightson-Winslow C. Assessment of myeloperoxidase activity in whole rat kidney. J Pharmacol Methods 1990;24:285–95.

[13] Theodorus P, Akerboom M, Sies H. Assay of glutathione, glutathione disulfide and glutathione mixed disulfides in biological samples. Meth Enzymol 1981;77:373–83.

[14] Buege AJ, Aust SD. Microsomal lipid peroxidation. Meth Enzymol 1978;52:302–10.

[15] Bradford MM. A rapid and sensitive method for the quantitation of microgram quantities of protein utilizing the principle of protein-dye binding. Anal Biochem 1976;72:248–54.

[16] Hasselgren PO. Prevention and treatment of ischemia of the liver. Surg Gynecol Obstet 1987;164:187–96.

[17] Dogan S, Aslan M. Hepatic ischemia-reperfusion injury and therapeutic strategies to alleviate cellular damage. Hepatology Res 2011;41:103–17.

[18] Dröge W. Free radicals in the physiological control of cell function. Physiol Rev 2002;82:47–95.

[19] Slyshenkov VS, Omelyanchik SN, Moiseenok AG, Trebukhina RV, Wojtczak L. Pantothenol protects rats against some deleterious effects of gamma radiation. Free Radic Biol Med 1998;24:894–9.

[20] Wojtczak L, Slyshenkov VS. Protection by pantothenic acid against apoptosis and cell damage by oxygen free radicals the role of glutathione. Biofactors 2003;17:61–73.

[21] Slyshenkov VS, Rakowska M, Moiseenok AG, Wojtczak L. Pantothenic acid and its derivatives protect Ehrlich ascites tumor cells against lipid peroxidation. Free Radic Biol Med 1995;19:767–72.

[22] Kumerova AO, Silova AA, Utno LY. Effect of pantethine on postheparinlipolytic activity and lipid peroxidation in the myocardium. Biull Eksp Biol Med 1991;111:33–5.

[23] Uysal HB, Dagli B, Yilmaz M, Kahyaoglu F, Gökçimen A, Omurlu IK, et al. Protective effects of dexpanthenol against acetaminophen-induced hepatorenal damage. Biomed Res 2017;28:740–9.

[24] Demirci B, Demir O, Dost T, Birincioglu M. Protective effect of vitamin B5 (dexpanthenol) on cardiovascular damage induced by streptozocin in rats. Bratisl Lek Listy 2014;115:190–6.

[25] Altintas R, Parlakpinar H, Beytur A, Vardi N, Polat A, Sagir M, et al. Protective effect of dexpanthenol on ischemia-reperfusion-induced renal injury in rats. Kidney Blood Press Res 2012;36:220–30.

[26] Kapp A, Zeck-Kapp G. Effect of Ca-pantothenate on human granulocyte oxidative metabolism. Allerg Immunol (Leipz) 1991;37:145–50.

[27] Ozansoy G, Akin B, Aktan F, Karasu Ç. Short-term gemfibrozil treatment reverses lipid profile and peroxidation but does not alter blood glucose and tissue antioxidant enzymes in chronically diabetic rats. Mol Cell Biochem 2001;216:59–63.

[28] Ceylan A, Karasu C, Aktan F, Güven C, Can B, Ozansoy G. Effects of simvastatin treatment on oxidant/antioxidant state and ultrastructure of diabetic rat myocardium. Gen Physiol Biophys 2003;22:535–47.